is rather close to the ratio of the transfer into $3d$ orbitals, namely, $B_0^2(A)/B_0^2(B) \simeq 2.6$. This is what one would expect qualitatively considering only the Fe-O distances.

In a subsequent publication we will discuss the difference in the A- and B-site hyperfine fields in ferrites and garnets as well as Fe^{3+} hyperfine fields measured in other compounds.

---

*Work supported by the Foundation for Fundamental Research of Matter (F.O.M.) of the Netherlands.

†National Research Council of Canada NATO Postdoctoral Fellow.

[1]G. A. Sawatzky, F. van der Woude, and A. H. Morrish, Phys. Rev. 187, 747 (1969); Phys. Letters 25A, 147 (1967); J. Appl. Phys. 39, 1204 (1968); in *Proceedings of the Conference on the Mössbaur Effect, Tihany*, 1969, edited by I. Densi (Hungarian Academy of Sciences, Budapest, 1971). p. 543.

[2]H. Abe, H. Matsura, H. Yasuoka, A. Hirai, T. Hashi, and T. Fukuyama, J. Phys. Soc. Japan 18, 1400 (1963).

[3]R. L. Streever and C. A. Uriano, Phys. Rev. 139, A305 (1965).

[4]I. S. Lyubutin, E. F. Makarov, and V. A. Povitskiĭ, Zh. Eksperim. i Teor. Fiz. 53, 65 (1968) [Sov. Phys. JETP 26, 44 (1968)].

[5]H. P. van de Braak and W. J. Caspers, Phys. Status Solidi 24, 733 (1967).

[6]J. Owen and D. R. Taylor, Phys. Rev. Letters 16, 1164 (1966).

[7]N. L. Huang, R. Orbach, and E. Simanek, Phys. Rev. Letters 17, 134 (1966).

[8]E. Simanek, N. L. Huang, and R. Orbach, J. Appl. Phys. 38, 1072 (1967).

[9]K. P. Belov and I. S. Lyubutin, Zh. Eksperim. i Teor. Fiz. Pis'ma v Redaktsiyu 1, 16 (1965) [Sov. Phys. JETP Letters 1, 16 (1965)].

[10]V. I. Goldanskii, M. N. Devisheva, V. A. Trukhtanov, and V. F. Belov, Zh. Eksperim. i Teor. Fiz. Pis'ma v Redaktsiyu 1, 19 (1965) [Sov. Phys. JETP Letters 1, 19 (1965)].

[11]B. J. Evans, in *Mössbauer Effect Methodology*, edited by I. J. Gruverman (Plenum, New York, 1968), Vol. 4, p. 139.

[12]V. I. Goldanskii, M. N. Devisheva, E. F. Makarov, G. V. Novikov, and V. A. Trukhtanov, Zh. Eksperim. i Teor. Fiz. Pis'ma v Redaktsiyu 4, 63 (1966) [Sov. Phys. JETP Letters 4, 42 (1966)].

[13]J. D. Litster and G. B. Benedek, J. Appl. Phys. 37, 1320 (1966).

[14]J. Sawicki, Czech. J. Phys. B 17, 371 (1967).

[15]R. W. Grant, H. Wiedersich, S. Geller, U. Gonser, and G. P. Espinosa, J. Appl. Phys. 38, 1455 (1967).

[16]J. P. Morel, J. Phys. Chem. Solids 28, 629 (1967).

[17]R. E. Watson (private communication).

[18]R. E. Watson, Phys. Rev. 111, 1108 (1958).

[19]E. Clementi, IBM J. Res. Develop. 9, 2 (1965).

[20]E. Simanek and Z. Sroubek, Phys. Rev. 163, 275 (1967).

[21]L. R. Walker, G. K. Wertheim, and V. Jaccarino, Phys. Rev. Letters 6, 98 (1961).

PHYSICAL REVIEW B VOLUME 4, NUMBER 9 1 NOVEMBER 1971

Parquet Diagrams in the Local-Moment Problem

R. A. Weiner
Department of Physics, Carnegie-Mellon University, Pittsburgh, Pennsylvania 15213
(Received 24 May 1971)

Parquet diagrams are used to self-consistently include vertex corrections to the paramagnon propagator in the Suhl model of local-moment formation. The equations are solved numerically in an approximation valid at high temperatures. Curie-law behavior for the self-consistent susceptibility is not found; instead the susceptibility varies roughly as $T^{-2/3}$. A conserving approximation to the susceptibility based on the parquet-diagram approximation for the mass operator is also investigated. This gives a susceptibility which diverges at finite T. Possible consequences of abandoning the high-temperature approximation are discussed.

I. INTRODUCTION

Suhl[1] has developed a model of local-moment formation based on the Anderson[2] or Wolff[3] models in which the strong intra-atomic Coulomb repulsion between localized d electrons of opposite spin, broadened by conduction-electron scattering, forms long-lived spin fluctuations in the localized state. The lifetime of the spin fluctuations, or localized paramagnons, is much longer than that of the d electrons themselves. At high temperatures this leads to a Curie-law susceptibility for the localized state, and at lower temperatures $\ln T$ behavior of the resistivity, reminiscent of the Kondo effect,[1,4,5] is found, though the Kondo temperature and the Curie constant predicted by this model are much smaller than is expected.[5] The model requires a self-consistent calculation of the d-electron propagator, renormalized by paramagnon exchange, and the paramagnon propagator, which is essential-

ly the electron vertex function. In previous calcalations the vertex function has been obtained from a Bethe-Salpeter equation in which the interaction is given by the bare potential U.[6] Béal-Monod and Mills[7] have shown that the inclusion of paramagnon exchange in the kernel of the Bethe-Salpeter equation has a significant effect on the paramagnon propagator and that this effect is at least as important as the self-energy corrections at low temperatures. This paper treats the problem of self-consistently calculating the paramagnon-exchange corrections by means of the parquet diagrams.[8]

In a preliminary version of this work[9] an approximate and relatively simple solution of the equations was found which led to a Curie-law susceptibility, i.e., $\chi \propto T^{-1}$. Two approximations were used: (i) The self-consistent paramagnon propagator was taken to have an infinite lifetime (this restricts the approximation of high temperatures); (ii) terms in the kernel of the effective Bethe-Salpeter equation for the paramagnon which introduced an extra frequency dependence were dropped. We shall relax the second approximation in this paper. The resulting equations are solved numerically. A drastic change in the behavior of the susceptibility as a function of temperature is found: $\chi \propto T^{-2/3}$ is the most singular low-temperature behavior of the solution.

We also investigate a conserving approximation to the susceptibility[10] based on this approximation to the mass operator in the hope that such an approximation, which gives the actual response to the external field for the approximate electron propagator we calculate, will give a more physical result for the susceptibility. We find that the conserving susceptibility is too singular—it diverges at finite temperatures, implying that either the parquet-diagram approximation has not succeeded in including all diagrams which lead to the Curie-law susceptibility in local-moment systems, or that the infinite-lifetime approximation has failed.

The parquet diagrams and equations are given in Sec. II, as well as the numerical results. The conserving approximation is derived and calculated in Sec. III. Section IV contains a discussion of the results and speculations as to what would occur if we were to relax the high-temperature approximation of zero-width paramagnons.

II. PARQUET DIAGRAMS

The paramagnon mode in this model appears as the nearly singular behavior, at low-frequency transfer, of the solution of a Bethe-Salpeter equation for the electron vertex function. Even though the solution is nearly singular, each term in the expansion of the vertex function is finite and well behaved. The problem of self-consistently calculating paramagnon-exchange effects in the effective interaction of this Bethe-Salpeter equation must then involve some way of coupling such nearly singular solutions of Bethe-Salpeter equations. The parquet diagrams[8] provide a formal method of expressing all diagrams for the vertex function in terms of the solutions of a set of coupled Bethe-Salpeter equations.[11] As the effective interaction for each of these Bethe-Salpeter equations is given in part by the solutions of the other equations in the set, the parquet diagrams thus generate one way of introducing the paramagnon-exchange effects self-consistently.

We classify a diagram as reducible if it can be broken into two disjoint parts by cutting two electron lines or an electron line and a hole line. Diagrams which cannot be so broken apart are totally irreducible. For particles interacting through a two-body potential there are three classes of reducible diagrams and no diagram is reducible in more than one channel. There are those diagrams reducible in the direct electron-hole channel, which we take to be those diagrams in which the electron and hole propagators are horizontal, as in Fig. 1(a), those reducible in the crossed electron-hole channel [Fig. 1(b)], and those reducible in the electron-electron channel [Fig. 1(c)]. All diagrams reducible in a particular channel may be summed by means of a Bethe-Salpeter equation, as shown in Fig. 1, in which the interaction part of the kernel is given by all diagrams irreducible in that channel, i.e., the totally irreducible diagrams plus all diagrams reducible in the other channels. If we let I be the totally irreducible part of the vertex function, γ^d the sum of all diagrams reducible in the direct channel, γ^c the sum of all diagrams reducible in the crossed channel, and γ^{ee} the sum of all diagrams reducible in the electron-electron channel, the corresponding Bethe-Salpeter equations, in the antisymmetrized many-body formalism,[12] are

$$\gamma^d = \beta^{-1} \sum I^d g g I^d + \beta^{-1} \sum I^d g g \gamma^d \,, \tag{1a}$$

$$\gamma^c = -\beta^{-1} \sum I^c g g I^c - \beta^{-1} \sum I^c g g \gamma^c \,, \tag{1b}$$

$$\gamma^{ee} = \tfrac{1}{2} \beta^{-1} \sum I^{ee} g g I^{ee} + \tfrac{1}{2} \beta^{-1} \sum I^{ee} g g \gamma^{ee} \,, \tag{1c}$$

$$I^d = I + \gamma^c + \gamma^{ee} \,,$$

$$I^c = I + \gamma^d + \gamma^{ee} \,,$$

$$I^{ee} = I + \gamma^d + \gamma^c \,,$$

where g stands for the electron propagator, and we have suppressed the spin and frequency arguments in the sums. The diagrams for γ^c may be obtained from those for γ^d by using the antisymmetry of the vertex function under the exchange of its electron (or hole) variables, which gives the crossing relations

$$\gamma^c_{\sigma_1,\sigma_2;\sigma_3,\sigma_4}(\epsilon, \epsilon'; \omega) = -\gamma^d_{\sigma_1,\sigma_2;\sigma_4,\sigma_3}(\epsilon, \epsilon+\omega; \epsilon'-\epsilon)$$

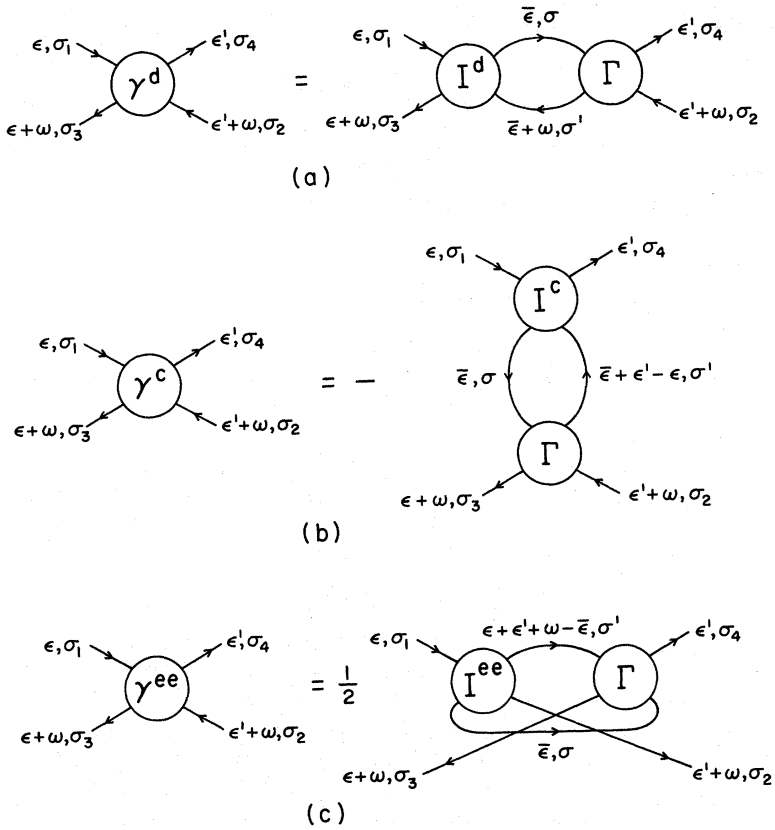

FIG. 1. The parquet diagrams. γ^d sums all diagrams reducible in the direct electron-hole channel, γ^c sums those reducible in the crossed electron-hole channel, and γ^{ee} sums those reducible in the electron-electron channel. The irreducible vertices I^d, I^c, and I^{ee} are the sums of all diagrams not reducible in their respective channels. The full vertex is $\Gamma = I + \gamma^d + \gamma^c + \gamma^{ee}$, where I is the totally irreducible vertex.

$$= -\gamma^d_{\sigma_2,\sigma_1;\sigma_3,\sigma_4}(\epsilon' + \omega, \epsilon', \epsilon - \epsilon') \,. \tag{2}$$

Both γ^{ee} and I are coupled to themselves by these crossing relations.

If we drop γ^c and γ^{ee} from I^d, and γ^d and γ^{ee} from I^c, and set I equal to the bare vertex, Eqs. (1) reduced to the vertex equation considered by Suhl[1] and the other work on this model,[4,5] which gives a vertex function which is nearly singular in the frequency transfer, which is ω for γ^d and $\epsilon' - \epsilon$ for γ^c. Therefore, we expect similar behavior for the parquet-diagram vertex functions. Unlike the Suhl vertex equation, the parquet equations cannot be solved in closed form. To self-consistently calculate the effects of paramagnon exchange, we must assume the existence of a paramagnonlike solution, i.e., a narrow resonance at $\omega = 0$ in γ^d and, from the crossing relations, at $\epsilon = \epsilon'$ in γ^c,[13] insert it into the effective interactions I^d, I^c, and I^{ee}, and obtain the same mode in the solution of the equations.

If we assume this mode to have a nonzero width the equations are still too complicated for reasonable numerical calculations. We therefore assume that for a first approximation we may take the mode to have zero width. Since we use the imaginary frequencies $i\omega_n = 2\pi i n/\beta$, the infinitely narrow mode is represented by a Kronecker δ, $\gamma^d \propto \delta_{\omega_n,0}$ and $\gamma^c \propto \delta_{\epsilon,\epsilon'}$. This approximation is reasonably valid at high temperatures where the imaginary frequencies are widely spaced.[14]

However, using $\gamma^c \propto \delta_{\epsilon,\epsilon'}$ in I^d yields a term in γ^d proportional to $\delta_{\epsilon,\epsilon'}$ itself, so that simplest approximation for γ^d which will be a self-consistent solution for zero-width paramagnon mode in γ^d and γ^c is

$$\gamma^d_{\sigma_1,\sigma_2;\sigma_3,\sigma_4}(\epsilon, \epsilon'; \omega) = G^1_{\sigma_1,\sigma_2;\sigma_3,\sigma_4}(\epsilon, \epsilon')\delta_{\omega,0} + G^2_{\sigma_1,\sigma_2;\sigma_3,\sigma_4}(\epsilon, \epsilon + \omega)\delta_{\epsilon,\epsilon'} \,, \tag{3}$$

where we assume G^1 and G^2 are slowly varying functions of their arguments. We shall also make the further approximation of replacing the totally irreducible vertex I by the bare vertex,

$$I_{\sigma_1,\sigma_2;\sigma_3,\sigma_4} = U(\delta_{\sigma_1,\sigma_3}\delta_{\sigma_2,\sigma_4} - \delta_{\sigma_1,\sigma_4}\delta_{\sigma_2,\sigma_3}) \,.$$

Since γ^c is related to γ^d by the crossing relations, I^{ee} is given in terms of U, G^1, and G^2, and Eq. (1c) gives I^d in terms of U, G^1, G^2, and the electron propagator g. Hence, Eq. (1a) becomes a self-consistent equation for G^1 and G^2.

The analysis is simplified by the use of the spin

projection operators appropriate for each channel:

$$\Lambda^{s}_{\sigma_1,\sigma_2;\sigma_3,\sigma_4}=\tfrac{1}{2}\,\delta_{\sigma_1,\sigma_3}\delta_{\sigma_2,\sigma_4}\ , \tag{4a}$$

$$\Lambda^{t}_{\sigma_1,\sigma_2;\sigma_3,\sigma_4}=\delta_{\sigma_1,\sigma_4}\delta_{\sigma_2,\sigma_3}-\tfrac{1}{2}\,\delta_{\sigma_1,\sigma_3}\delta_{\sigma_2,\sigma_4} \tag{4b}$$

for the direct channel and

$$\Lambda^{\pm}_{\sigma_1,\sigma_2;\sigma_3,\sigma_4}=\tfrac{1}{2}\,(\delta_{\sigma_1,\sigma_4}\delta_{\sigma_2,\sigma_3}\pm\delta_{\sigma_1,\sigma_3}\delta_{\sigma_2,\sigma_4}) \tag{5}$$

for the electron-electron channel. Decomposing G^1, G^2, and γ^{ee} according to

$$G^{i}_{\sigma_1,\sigma_2;\sigma_3,\sigma_4}(\epsilon,\epsilon')=G^{i}_{s}(\epsilon,\epsilon')\Lambda^{s}_{\sigma_1,\sigma_2;\sigma_3,\sigma_4}+G^{i}_{t}(\epsilon,\epsilon')\Lambda^{t}_{\sigma_1,\sigma_2;\sigma_3,\sigma_4}\ , \tag{6}$$

$$\gamma^{ee}_{\sigma_1,\sigma_2;\sigma_3,\sigma_4}(\epsilon,\epsilon';\omega)=\gamma_{+}(\epsilon,\epsilon';\omega)\Lambda^{+}_{\sigma_1,\sigma_2;\sigma_3,\sigma_4}+\gamma_{-}(\epsilon,\epsilon';\omega)\Lambda^{-}_{\sigma_1,\sigma_2;\sigma_3,\sigma_4}\ , \tag{7}$$

we have

$$\gamma_{\pm}(\epsilon,\epsilon';\omega)=R_{\pm}(\epsilon,\epsilon';\omega)+\beta^{-1}g(\epsilon)g(\epsilon'+\omega)\times\overline{G}^{2}_{\pm}(\epsilon,\epsilon'+\omega)A_{\pm}(\epsilon,\epsilon'+\omega)[\,\delta_{\epsilon,\epsilon'}\mp\delta_{\omega,0}]\ , \tag{8}$$

$$A_{\pm}(\epsilon,\epsilon')=[1-\beta^{-1}g(\epsilon)g(\epsilon')\overline{G}_{\pm}(\epsilon,\epsilon')]^{-1}\ , \tag{9}$$

where

$$\overline{G}_{+}=-\tfrac{1}{2}\,(G^1_s+G^1_t-G^2_s-G^2_t)\ , \tag{10a}$$

$$\overline{G}_{-}=\tfrac{1}{2}\,(3G^1_t-G^1_s+3G^2_t-G^2_s) \tag{10b}$$

(we have dropped the frequency arguments of the $\overline{G}$'s and G^i's) and

$$R_{+}(\epsilon,\epsilon';\omega)=0\ , \tag{11a}$$

$$R_{-}(\epsilon,\epsilon';\omega)=2U\{1-A_{-}(\epsilon,\epsilon'+\omega)A_{-}(\epsilon',\epsilon+\omega)\times[1+S_{-}(\epsilon+\epsilon'+\omega)]^{-1}\}\ , \tag{11b}$$

$$S_{-}(\omega)=\frac{U}{\beta}\sum_{\bar\epsilon}g(\bar\epsilon)g(\omega-\bar\epsilon)A_{-}(\bar\epsilon,\omega-\bar\epsilon)\ .$$

By using the free propagators g_0 and setting $A_-=1$, we have $S^0_-(0)>0$. We do not expect the sign of S_- to change when we use the self-consistent g's and the correct expression for A_-, so that the $R_\pm$ terms in Eq. (8) do not contribute to the singular behavior of γ^{ee} and have been dropped in the subsequent analysis.

Defining the auxiliary quantities

$$Q_{\pm}(\epsilon,\epsilon')=\beta^{-1}g(\epsilon)g(\epsilon')\overline{G}^{2}_{\pm}(\epsilon,\epsilon')A_{\pm}(\epsilon,\epsilon')\ , \tag{12}$$

$$Q^1_s=-\tfrac{1}{2}\,(3Q_{+}+Q_{-}+G^2_s+3G^2_t)\ , \tag{13a}$$

$$Q^1_t=\tfrac{1}{2}\,(Q_{-}-Q_{+}+G^2_t-G^2_s)\ , \tag{13b}$$

$$Q^2_s=\tfrac{1}{2}\,(3Q_{+}-Q_{-}-G^1_s-3G^1_t)\ , \tag{13c}$$

$$Q^2_t=\tfrac{1}{2}\,(Q_{+}+Q_{-}+G^1_t-G^1_s) \tag{13d}$$

(again dropping the frequency arguments), we find, using Eqs. (2) and (8), that G^1 and G^2 satisfy

$$G^1_s(\epsilon,\epsilon')=\gamma_s(\epsilon,\epsilon')-U-Q^1_s(\epsilon,\epsilon')\ , \tag{14a}$$

$$G^1_t(\epsilon,\epsilon')=\gamma_t(\epsilon,\epsilon')+U-Q^1_t(\epsilon,\epsilon')\ , \tag{14b}$$

$$G^2_s(\epsilon,\epsilon')=\beta^{-1}g(\epsilon)g(\epsilon')[Q^2_s(\epsilon,\epsilon')]^2\times[1-\beta^{-1}g(\epsilon)g(\epsilon')Q^2_s(\epsilon,\epsilon')]^{-1}\ , \tag{15a}$$

$$G^2_t(\epsilon,\epsilon')=\beta^{-1}g(\epsilon)g(\epsilon')[Q^2_t(\epsilon,\epsilon')]^2\times[1-\beta^{-1}g(\epsilon)g(\epsilon')Q^2_t(\epsilon,\epsilon')]^{-1}\ , \tag{15b}$$

where the γ's must satisfy

$$\gamma_s(\epsilon,\epsilon')=[U+Q^1_s(\epsilon,\epsilon')]A_s(\epsilon)A_s(\epsilon')+A_s(\epsilon)\beta^{-1}\times\textstyle\sum_{\bar\epsilon}[U+Q^1_s(\epsilon,\bar\epsilon)]g^2(\bar\epsilon)\gamma_s(\bar\epsilon,\epsilon')\ , \tag{16a}$$

$$\gamma_t(\epsilon,\epsilon')=[-U+Q^1_t(\epsilon,\epsilon')]A_t(\epsilon)A_t(\epsilon')+A_t(\epsilon)\beta^{-1}\times\textstyle\sum_{\bar\epsilon}[-U+Q^1_t(\epsilon,\bar\epsilon)]g^2(\bar\epsilon)\gamma_t(\bar\epsilon,\epsilon')\ , \tag{16b}$$

$$A_s(\epsilon)=[1-\beta^{-1}g^2(\epsilon)Q^2_s(\epsilon,\epsilon)]^{-1}\ , \tag{17a}$$

$$A_t(\epsilon)=[1-\beta^{-1}g^2(\epsilon)Q^2_t(\epsilon,\epsilon)]^{-1}\ . \tag{17b}$$

If we drop the Q^1's and the A's, Eqs. (16a) and (16b) reduce to the singlet and triplet vertex functions, respectively, without paramagnon exchange.[1,4] Therefore, it is more convenient to take $\overline{\gamma}_s=\gamma_s-U$ and $\overline{\gamma}_t=\gamma_t+U$ as the basic quantities of the theory, solve for Q^1 and Q^2 in terms of the $\overline{\gamma}$'s and so convert Eqs. (16) into coupled nonlinear equations for the γ's. From Eqs. (10), (13), and (14) we have

$$\overline{\gamma}_s+\overline{\gamma}_t=-2(\overline{G}_{+}+Q_{+})\ , \tag{18a}$$

$$3\overline{\gamma}_t-\overline{\gamma}_s=2(Q_{-}-\overline{G}_{-})\ , \tag{18b}$$

$$\overline{\gamma}_s-\overline{\gamma}_t=-2(Q^2_t+G^2_t)\ , \tag{18c}$$

$$3\overline{\gamma}_t-\overline{\gamma}_s=-2(Q^2_s+G^2_s)\ . \tag{18d}$$

Using Eqs. (12) and (15), and letting gg' stand for $g(\epsilon)g(\epsilon')$, Eqs. (18) yield

$$Q_{+}=\beta^{-1}gg'[\tfrac{1}{2}\,(\overline{\gamma}_s+\overline{\gamma}_t)]^2[1-\tfrac{1}{2}\,\beta^{-1}gg'(\overline{\gamma}_s+\overline{\gamma}_t)]^{-1}\ , \tag{19a}$$

$$Q_{-}=\beta^{-1}gg'[\tfrac{1}{2}\,(3\overline{\gamma}_t-\overline{\gamma}_s)]^2[1+\tfrac{1}{2}\,\beta^{-1}gg'(3\overline{\gamma}_t-\overline{\gamma}_s)]^{-1}\ , \tag{19b}$$

$$G^2_t=\beta^{-1}gg'[\tfrac{1}{2}\,(\overline{\gamma}_t-\overline{\gamma}_s)]^2[1+\tfrac{1}{2}\,\beta^{-1}gg'(\overline{\gamma}_t-\overline{\gamma}_s)]^{-1}\ , \tag{19c}$$

$$G^2_s=\beta^{-1}gg'[\tfrac{1}{2}\,(3\overline{\gamma}_t+\overline{\gamma}_s)]^2[1-\tfrac{1}{2}\,\beta^{-1}gg'(3\overline{\gamma}_t+\overline{\gamma}_s)]^{-1}\ . \tag{19d}$$

Equations (18) and (19), combined with Eqs. (17), also give

$$A_s(\epsilon)=1-\tfrac{1}{2}\,\beta^{-1}g^2(3\overline{\gamma}_t+\overline{\gamma}_s)\ , \tag{20a}$$

$$A_t(\epsilon)=1+\tfrac{1}{2}\,\beta^{-1}g^2(\overline{\gamma}_t-\overline{\gamma}_s)\ . \tag{20b}$$

Having determined the $Q_\pm$'s and the G^2's in terms

of the $\bar{\gamma}$'s and hence the γ's, we can find the Q^1's in terms of the γ's from Eqs. (13). Along with the A's as given by Eqs. (20), this determines the effective interactions in the Bethe-Salpeter equations, Eqs. (16), for the strength of the zero-width paramagnon mode (the γ's) in terms of the γ's themselves, i.e., we have obtained a self-consistent coupling of paramagnon exchange in the effective interaction with the equations for the paramagnon's existence.

The final step in the calculation is to express the mass operator in terms of the γ's and the propagator g. Using the spin decomposition in the direct channel, the full vertex $\Gamma = I + \gamma^d + \gamma^c + \gamma^{ee}$ is

$$\Gamma_s(\epsilon, \epsilon'; \omega) \simeq \delta_{\omega,0}\gamma_s(\epsilon, \epsilon') + \delta_{\epsilon,\epsilon'} Q_s^2(\epsilon, \epsilon+\omega) \times [1 - \beta^{-1} g(\epsilon) g(\epsilon+\omega) Q_s^2(\epsilon, \epsilon+\omega)]^{-1} , \tag{21a}$$

$$\Gamma_t(\epsilon, \epsilon'; \omega) \simeq \delta_{\omega,0}\gamma_t(\epsilon, \epsilon') + \delta_{\epsilon,\epsilon'} Q_t^2(\epsilon, \epsilon+\omega) \times [1 - \beta^{-1} g(\epsilon) g(\epsilon+\omega) Q_t^2(\epsilon, \epsilon+\omega)]^{-1} , \tag{21b}$$

where we have kept only those terms which have Kronecker-δ singularities in the frequency transfers. From Eqs. (18), (19), and (13) we can find the Q^2's in terms of the $\bar{\gamma}$'s, so that

$$\Gamma_s(\epsilon, \epsilon'; \omega) = \gamma_s(\epsilon, \epsilon')\delta_{\omega,0} - \tfrac{1}{2}[3\bar{\gamma}_t(\epsilon, \epsilon+\omega) + \bar{\gamma}_s(\epsilon, \epsilon+\omega)]\delta_{\epsilon,\epsilon'} , \tag{22a}$$

$$\Gamma_t(\epsilon, \epsilon'; \omega) = \gamma_t(\epsilon, \epsilon')\delta_{\omega,0} + \tfrac{1}{2}[\bar{\gamma}_t(\epsilon, \epsilon+\omega) - \bar{\gamma}_s(\epsilon, \epsilon+\omega)]\delta_{\epsilon,\epsilon'} . \tag{22b}$$

We calculate the mass operator (minus the Hartree-Fock term) for the diagram of Fig. 2, obtaining

$$\Sigma(\epsilon) = -\frac{1}{4} g(\epsilon) \frac{U}{\beta^2} \sum_{\bar{\epsilon}} g(\bar{\epsilon})[\gamma_s(\epsilon, \bar{\epsilon}) + \bar{\gamma}_s(\epsilon, \bar{\epsilon}) - 3\gamma_t(\epsilon, \bar{\epsilon}) - 3\bar{\gamma}_t(\epsilon, \bar{\epsilon})] , \tag{23}$$

which completes our coupled equations for the vertex functions and the propagator.

To find out what the effects of paramagnon exchange are we now investigate the changes in the effective interaction due to the Q^1's and the A's. The case where Q^1's are dropped and only the A's kept has already been studied[9]: The parquet equations then lead to slight but significant changes from Suhl's original results.[1] Keeping the Q^1's, however, leads to drastic changes. The expressions for Q_s^1 and Q_t^1 can be simplified by noting that for both the Suhl vertex[1] and the preliminary investigation of the parquet diagrams[9] $\gamma_s \lesssim U$ while $|\gamma_t| \gg U$. Only when $|\gamma| \gg U$ is the assumption that the vertex function can be approximated by a Kronecker δ valid, so that keeping only $\bar{\gamma}_t \simeq \gamma_t$, we have

$$Q_s^1 = -3\beta^{-1} g g' \gamma_t^2 [1 - \tfrac{3}{4}(\beta^{-1} g g' \gamma_t)^2] \times [1 - \tfrac{1}{4}(\beta^{-1} g g' \gamma_t)^2]^{-1} [1 - \tfrac{9}{4}(\beta^{-1} g g' \gamma_t)^2] , \tag{24a}$$

$$Q_t^1 = -\tfrac{7}{2}(\beta^{-1} g g')^2 \gamma_t^3 [1 - \tfrac{9}{28}(\beta^{-1} g g' \gamma_t)^2] \times [1 - \tfrac{1}{4}(\beta^{-1} g g' \gamma_t)^2]^{-1} [1 - \tfrac{9}{4}(\beta^{-1} g g' \gamma_t)^2]^{-1} . \tag{24b}$$

From the Dyson equation

$$g^{-1}(\epsilon) = g_0^{-1}(\epsilon) - \Sigma(\epsilon) ,$$

we can show for the case $\epsilon_d = -\frac{1}{2} U$ that g, with the Hartree-Fock term included in the mass operator,[15] is a pure imaginary and odd function of the imaginary fermion frequencies $i\epsilon_n = (2n+1)\pi i/\beta$. It then follows that $\gamma_t(\epsilon_n, \epsilon_{n'})$ is negative and that $Q_t^1(\epsilon_n, \epsilon_{n'})$ is positive for all values of ϵ_n and $\epsilon_{n'}$. That is, the part of the effective interaction which is due to paramagnon exchange reduces the effective interaction below that of the bare potential U and hence makes the paramagnon mode less likely to occur. One may estimate how strong the modification is by noting that the condition determining the low-temperature behavior is now Q_t^1 finite, whereas in earlier work[1,9] the condition was Σ finite, which leads to $\gamma_t/\beta \simeq \gamma_t T$ finite as $T \to 0$. Assuming that the low-temperature propagators are virtually temperature independent, as is true in the earlier work,[1,9] Eq. (24b) implies

$$\gamma_t^3/\beta^2 \to \text{const} ,$$

as $T \to 0$, or $\gamma_t \propto \beta^{2/3} \propto T^{-2/3}$ in the full zero-width parquet approximation. Since the susceptibility is given by

$$\chi = -(g\mu_B)^2 \left(\frac{1}{\beta^2} \sum_{\epsilon,\epsilon'} g^2(\epsilon) g^2(\epsilon') \gamma_t(\epsilon, \epsilon') + \frac{1}{2\beta^2} \sum_{\epsilon} g^4(\epsilon)[\bar{\gamma}_t(\epsilon, \epsilon) - \bar{\gamma}_s(\epsilon, \epsilon)] \right) , \tag{25}$$

this leads to $\chi \propto T^{-2/3}$ in contrast to the Curie-law susceptibility $\chi \propto T^{-1}$ found before.

The effect of paramagnon exchange on the scalar vertex is more difficult to ascertain, since Q_s^1, as given by Eq. (24a), does not have a definite sign. It is positive when ϵ and ϵ' are on the same side of the real axis and negative when they are on opposite sides. (A positive Q_s^1 increases the effective repulsion in the scalar vertex equation.) To verify our assumption that $\gamma_s < U$, the numerical calculations solved the linear equation for γ_s, Eq. (16a), as well as the nonlinear triplet equation with Q_s^1

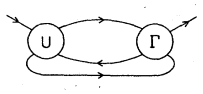

FIG. 2. The mass operator. U is the bare two-body interaction.

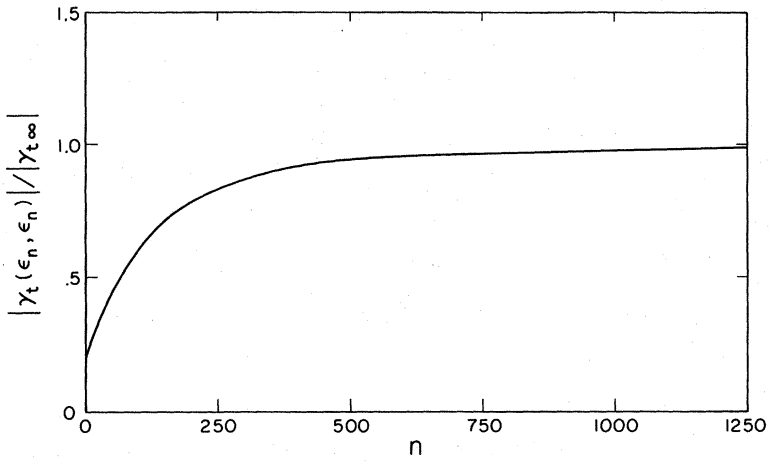

FIG. 3. $|\gamma_t(\epsilon_n,\epsilon_n)|/\gamma_{t\infty}, \epsilon_n=(2n+1)\times\pi i/\beta$, as a function of n for $U=3\ U_c=9.42$ and $\beta=100$. The maximum value of n in the calculation is 15 000, and the asymptotic value of the vertex $\gamma_{t\infty}$ is 450. The condition $|\gamma_t(\epsilon_n,\epsilon_n)| \gg U$ is always satisfied. (All energies are measured in units of Δ, the width of the unrenormalized d-state propagator.)

and Q_t^1 given by Eqs. (24). This was solved self-consistently with Dyson's equation for the propagator, the mass operator being given by Eq. (23), with $\bar{\gamma}_t$ set equal to γ_t and γ_s set equal to zero. The frequencies ϵ and ϵ' were picked on an exponentially spaced mesh, and sums were performed by linear interpolation between mesh points. The solution procedure is to guess an input $g(\epsilon)$ and $\gamma_t(\epsilon,\epsilon')$. The right-hand side of Eq. (16b) is then calculated, giving an output $\gamma_t(\epsilon,\epsilon')$, and a new input γ_t is guessed. This process is repeated for a fixed $g(\epsilon)$ until convergence is obtained; then the mass operator is calculated, a new input g obtained, and the process repeated until a solution is found for both g and γ_t. The frequency mesh is then refined and the procedure repeated until convergence is obtained as a function of the fineness of the frequency mesh. At the lowest temperatures and highest values of U, we obtain 5% convergence; at higher temperatures and for smaller values of U, the convergence is better, usually within 2%. After a converged solution is found for γ_t, the scalar vertex is obtained by matrix inversion. The condition $\gamma_s < U$ is always satisfied. The susceptibility is then calculated from Eq. (25).

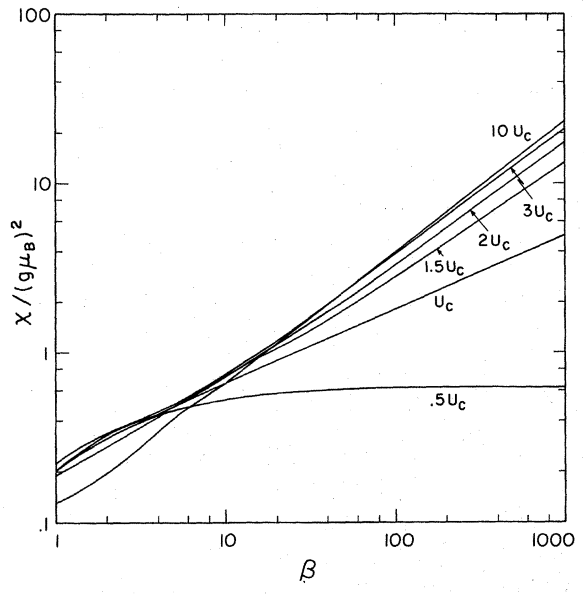

FIG. 4. The self-consistent susceptibility χ as a function of β for various values of U.

A typical plot of $\gamma_t(\epsilon,\epsilon)/\gamma_{t\infty}$, where $\gamma_{t\infty}$ is the asymptotic value of $\gamma_t(\epsilon,\epsilon)$ as $\epsilon\to-\infty$, is shown in Fig. 3. The frequency dependence is quite striking and arises from the fact that Q_t^1 is largest at the smallest frequencies where the propagator is largest. In general, the condition $|\gamma_{t\infty}| \gg U$ is satisfied quite well, but the corresponding condition for low frequencies is not so well satisfied, especially for large U.

The solution for the susceptibility as a function of $\beta=(kT)^{-1}$ is plotted in Fig. 4. For $U \geq U_c=\pi\Delta/A^2$, where Δ and A are the width and strength, respectively, of the d-state resonance in the unrenormalized propagator,[1] χ behaves as β^α at low temperatures, with $\alpha=0.44$ for $U=U_c$ and increasing from 0.69 to 0.76 as U increases from $1.5U_c$ to $10U_c$. This temperature dependence for the self-consistent susceptibility is unsatisfactory for a theory of local-moment formation. In Sec. III we will consider a different way of calculating the susceptibility in the framework of the parquet-diagram approximation and see that it too leads to unsatisfactory temperature dependence for χ, but of a completely different nature.

III. CONSERVING APPROXIMATIONS TO THE SUSCEPTIBILITY

An alternative way of calculating the susceptibility, given a particular approximation for the propagator, is by the conserving approximations of Baym and Kadanoff.[10] These approximations are

such that for a given approximation to the propagator they generate space- and time-dependent response functions, of which the susceptibility is one, which obey local conservation laws for the number, charge current, spin current, and energy densities. They are derived in a physically attractive way: A given approximation to the dynamics of the particles, i.e., the mass operator, is formally calculated in the presence of an external field, and the equations for the linear response functions appropriate for this approximation are obtained by taking the first derivative of the propagator with respect to the field and then setting the field equal to zero. In this way, the conserving approximation gives the actual linear response of the approximation to the single-particle dynamics.[16] In this section we will derive the conserving approximations to the susceptibility for both the Suhl vertex function and the parquet vertex, and investigate the effect on the susceptibility in the zero-width approximation to the self-consistent vertex functions.

A. Suhl Vertex

Following the prescription of Baym and Kadanoff,[10] the diagrammatic equation for the conserving vertex function for the Suhl self-consistent vertex is shown in Fig. 5. We have set the frequency transfer ω equal to zero, as we are interested in the static susceptibility; the only remaining frequency is the electron frequency ϵ. Using a spin decomposition to pick out the triplet vertex, which is all that contributes to the susceptibility, and keeping only the triplet part of the self-consistent vertex, we have

$$\Gamma_c(\epsilon) = -1 - \frac{1}{\beta}\sum_{\bar{\epsilon}} g^2(\bar{\epsilon}) \Big\{ U + \tfrac{1}{2}\bar{\gamma}(\bar{\epsilon}-\epsilon) + \frac{1}{\beta}\sum_{\epsilon'} g(\epsilon')\gamma(\epsilon'-\epsilon)\big[g(\bar{\epsilon}+\epsilon'-\epsilon)(\gamma(\epsilon'-\epsilon)-\tfrac{1}{2}U) - g(\bar{\epsilon}+\epsilon-\epsilon')(\gamma(\epsilon'-\epsilon)+\tfrac{1}{2}U)\big] \Big\} \Gamma_c(\bar{\epsilon}) , \tag{26}$$

where γ, given by

$$\gamma(\omega) = U/[1-S(\omega)],$$

$$\bar{\gamma}(\omega) = US(\omega)/[1-S(\omega)],$$

$$S(\omega) = -\frac{U}{\beta}\sum_{\epsilon} g(\epsilon) g(\epsilon+\omega) ,$$

is the self-consistent triplet vertex. Going to the zero-width approximation,

$$\gamma(\omega) \simeq \gamma(0)\delta_{\omega,0} = \gamma\delta_{\omega,0} ,$$

we have, for $\epsilon_d = -\frac{1}{2}U$, so that g is odd in ϵ,

$$\Gamma_c(\epsilon) = -1 - \frac{\bar{\gamma}}{2\beta} g^2(\epsilon)\Gamma_c(\epsilon) - \frac{U}{\beta}\sum_{\bar{\epsilon}} g^2(\bar{\epsilon})\Gamma_c(\bar{\epsilon}) ,$$

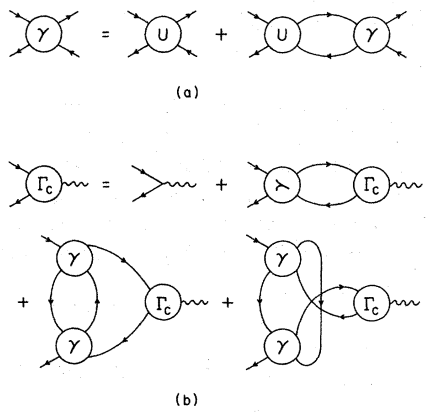

FIG. 5. (a) The Suhl self-consistent vertex equation. (b) The equation for the vertex function in the conserving approximation.

$$\bar{\gamma} = \gamma - U , \tag{27}$$

which is readily solved, giving the conserving susceptibility

$$\chi_c = (g\mu_B)^2 S'/[U(1-S')] , \tag{28}$$

$$S' = -\frac{U}{\beta}\sum_{\epsilon} g^2(\epsilon)\left(1+\frac{1}{2}\beta^{-1}\bar{\gamma}g^2(\epsilon)\right)^{-1} . \tag{29}$$

Since $g^2 < 0$ for $\epsilon_d = -\frac{1}{2}U$, $S' > S(0)$. As the self-consistency condition at $T=0$ is $S(0)=1$, $S'(T=0) > 1$ and so for some $T>0$, $S'=1$, i.e., χ_c is divergent at a nonzero temperature. This result is of course nonphysical, and the conclusion which must be drawn from it is that the Suhl vertex omits a class of diagrams which are essential for the correct description of local-moment formation.

B. Parquet Vertex

With the parquet vertex we have tried to include many of the paramagnon-exchange vertex diagrams. In doing so we have also included the diagrams which led to the divergence of the Suhl conserving susceptibility. We may then hope that these are the missing diagrams in the calculation of the conserving susceptibility.

It is extremely difficult to obtain a diagrammatic representation of the conserving vertex function in this case, as the parquet diagrams themselves are quite complicated. Therefore, we have derived a set of self-consistent equations in the zero-width approximation to the parquet diagrams for an applied external magnetic field. The spin decompositions of Sec. II are no longer valid, and we cannot simplify these equations so they have the form of simple Bethe-Salpeter equations. However, we may linearize the equations with respect to the spin- and field-dependent part of the propagator by writing

$$g_\sigma^{-1}(\epsilon) = g^{-1}(\epsilon) + \sigma \delta g^{-1}(\epsilon) , \tag{30}$$

where to lowest order δg^{-1} is first order in the external field H and g^{-1} is zeroth order. The solution of the linearized self-consistent vertex equations is then inserted into the mass operator, which is again linearized, and hence a linear equation for δg^{-1} is obtained. The susceptibility is found from

$$\chi = -(g\mu_B)^2 \frac{1}{\beta} \sum_\epsilon g^2(\epsilon) \lim_{H \to 0} \frac{\delta g^{-1}(\epsilon)}{g\mu_B H} . \tag{31}$$

The derivation of the equation for

$$\Gamma_c(\epsilon) = \lim_{H \to 0} \frac{\delta g^{-1}(\epsilon)}{g\mu_B H}$$

is then merely a problem of complicated and tedious algebraic manipulations which we shall not go through here. Using $|\gamma_t| \gg \gamma_s$ and U, we obtain

$$\Gamma_c(\epsilon) = \left[1 - \frac{U}{\beta} \sum_{\bar\epsilon} g^2(\bar\epsilon) \left(1 + \frac{1}{\beta} g(\epsilon) g(\bar\epsilon) \gamma(\epsilon, \bar\epsilon)\right) \Gamma_c(\bar\epsilon) + \frac{U}{\beta^2} g(\epsilon) \sum_{\bar\epsilon} g^2(\bar\epsilon) \left(\frac{\partial\gamma(\bar\epsilon, \epsilon)}{\partial H} - \frac{\partial\gamma(\epsilon, \bar\epsilon)}{\partial H}\right)\right] \times \left(1 + \frac{1}{2} \frac{U}{\beta} g^2(\epsilon) \frac{1}{\beta} \sum_{\bar\epsilon} g^2(\bar\epsilon) \gamma(\bar\epsilon, \epsilon)\right)^{-1} , \tag{32}$$

where γ and g are the solutions of the parquet equations, and

$$\begin{aligned} \frac{\partial\gamma}{\partial H}(\epsilon, \epsilon') = {} & \left(3A_t(\epsilon)[-U + Q_t^1(\epsilon, \epsilon')] \frac{1}{\beta} \gamma(\epsilon', \epsilon') g^3(\epsilon') \Gamma_c(\epsilon') \right. \\ & - A_t(\epsilon) A_s(\epsilon') \left\{ x\gamma_t(\epsilon, \epsilon') \left[\left(1 - \frac{x^2}{2} + \frac{9}{16} x^4\right) g(\epsilon) \Gamma_c(\epsilon) + x \left(1 + \frac{3}{4} x^2\right) g(\epsilon') \Gamma_c(\epsilon')\right] + x\left(2 - \frac{5}{2} x^2\right) \frac{\partial\gamma}{\partial H}(\epsilon', \epsilon)\right\} \\ & \times \left(1 - \frac{1}{4} x^2\right)^{-1} \left(1 - \frac{9}{4} x^2\right)^{-1} + A_t(\epsilon) \frac{1}{\beta} \sum_{\bar\epsilon \neq \epsilon'} [-U + Q_t^1(\epsilon, \bar\epsilon)] g^2(\bar\epsilon) \frac{\partial\gamma}{\partial H}(\bar\epsilon, \epsilon')\Big) \\ & \times \left[1 + A_t(\epsilon) A_s(\epsilon') x^2 \left(\frac{5}{2} - \frac{11}{4} x^2 + \frac{9}{32} x^4\right)\left(1 - \frac{1}{4} x^2\right)^{-1} \left(1 - \frac{9}{4} x^2\right)^{-1}\right], \end{aligned}$$

$$x = (1/\beta) g(\epsilon) g(\epsilon') \gamma(\epsilon, \epsilon'). \tag{33}$$

Though this is a linear equation for Γ_c and can be solved numerically by matrix inversion, the computational work involved is not worth the effort. A low-temperature approximation may be derived which reveals the essential features of the conserving susceptibility.

This approximation is derived by noting that if $\gamma \propto \beta^{2/3}$ for large β, then $x \propto \beta^{-1/3}$ and many of the terms in Eqs. (32) and (33) will drop out. Assuming that a frequency sum will give a contribution of order β times the average magnitude of the summand, we obtain

$$\Gamma_c(\epsilon) = \left[1 - \frac{U}{\beta} \sum_{\bar\epsilon} g^2(\bar\epsilon) \left(1 - \frac{x^2}{2\beta} \sum_{\epsilon'} g^2(\epsilon') \gamma(\epsilon', \bar\epsilon)\right) \Gamma_c(\bar\epsilon)\right] \times \left[1 + \frac{U}{2\beta} g^2(\epsilon) \frac{1}{\beta} \sum_{\bar\epsilon} g^2(\bar\epsilon) \gamma(\epsilon, \bar\epsilon) \left(1 - \frac{x^2}{\beta} \sum_{\epsilon'} g^2(\epsilon') \gamma(\epsilon', \bar\epsilon)\right)\right]^{-1} ,$$

$$x = g(\epsilon) g(\bar\epsilon) \gamma(\epsilon, \bar\epsilon)/\beta . \tag{34}$$

Comparing this with the equation for γ_t at low temperatures, we see that the leading term in Q_t^1 ,

$$\tfrac{1}{2} [g(\epsilon) g(\bar\epsilon)/\beta]^2 \gamma^3(\epsilon, \bar\epsilon) ,$$

has been replaced by

$$-\frac{1}{2} \left(\frac{g(\epsilon) g(\bar\epsilon) \gamma(\epsilon, \bar\epsilon)}{\beta}\right)^2 \frac{U}{\beta} \sum_{\epsilon'} g^2(\epsilon') \gamma(\epsilon', \bar\epsilon)$$

in Eq. (34). We expect this term to be of the same order of magnitude as the leading term in Q_t^1, i.e., essentially temperature independent at low T, but whether the sum

$$-\frac{U}{2\beta} \sum_{\epsilon'} g^2(\epsilon') \gamma(\epsilon', \bar\epsilon)$$

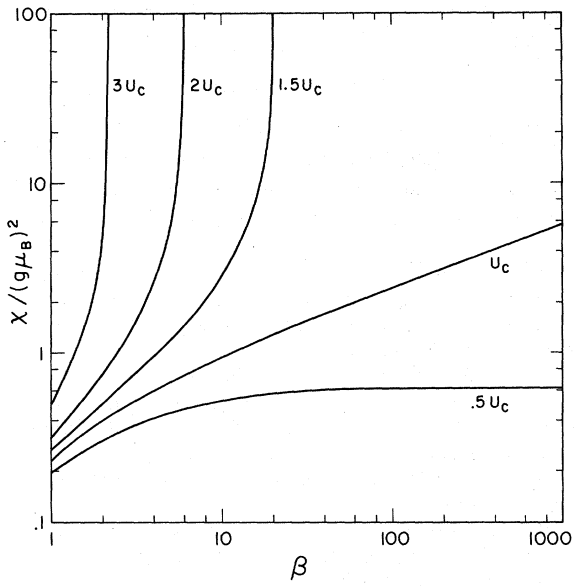

FIG. 6. The conserving approximation susceptibility as a function of β for various values of U. The results for $U \leq U_c$ agree exactly with the self-consistent susceptibility at low temperatures, and χ_c for $U = 10U_c$ diverges for $\beta < 1$.

is larger or smaller than $\frac{1}{2}\gamma(\epsilon, \bar{\epsilon})$ is not obvious. If it is smaller, the effective interaction in Eq. (34) will be stronger than that in Eq. (16b) and we expect the conserving susceptibility to diverge, while if it is larger, the effective interaction will be weaker, and thus the conserving susceptibility should in fact be finite at $T = 0$. Indeed, it is not at all clear what conditions on γ must be satisfied for Eq. (34) to yield a susceptibility that diverges exactly at $T = 0$, i.e., proportional to $T^{-\alpha}$ at low temperatures.

The numerical solution of Eq. (34), shown in Fig. 6, provides the answer to these questions for $U_c \leq U \leq 10\,U_c$: The effective interaction is stronger and the conserving susceptibility diverges at finite T. This conclusion has been verified by the solution of the full equations for Γ_c, Eqs. (32) and (33), in the region of the divergence. Hence, the parquet-diagram approximation, at least when coupled with the zero-width assumption for the paramagnon mode, does not yield a physically consistent picture of the mechanism of local-moment formation.

IV. DISCUSSION

There are two ways of understanding the failure of the preceding parquet-diagram calculations to give a tenable theory of local-moment formation: Either important classes of diagrams have been left out, or the zero-width assumption for the paramagnon mode is unrealistic. If the first case is true, it seems unlikely that any diagrammatic theory of local-moment formation will work, i.e., the coupling between paramagnon modes in the parquet-diagram scheme must be included, and so higher-order approximations in the totally irreducible vertex are the only extension of the theory available. As this will be an essentially perturbative expansion, it does not seem likely that anything other than the full series for I will be sufficient.

If it is the case that the zero-width assumption is at the root of the problems with the previous calculations, we may speculate as to the effects to allowing the paramagnon mode to have a finite width, as in Levine and Suhl[4] and Hamann.[5] We expect γ^d to have narrow modes at $\omega = 0$ and at $\epsilon = \epsilon'$, corresponding to the $\delta_{\omega,0}$ and $\delta_{\epsilon,\epsilon'}$ terms in the zero-width approximation. However, the $\epsilon = \epsilon'$ mode should be broader and weaker than the $\omega = 0$ mode since it will arise from sums over overlapping $\omega = 0$ modes in the inhomogeneous term in Eq. (1a). This is seen explicitly in Eqs. (13) and (15), where the self-consistent G^2's are proportional to $(G^1)^2$. Since the Q^1's in the equations for γ_s and γ_t arise from these $\epsilon = \epsilon'$ singularities, this means that the reduction of the triplet effective interaction will be comparatively weaker than it has been in the zero-width approximation. However, the reduction of the triplet effective interaction would still have significant effects. Since paramagnon exchange in the vertex function tends to weaken the enhancement of the self-consistent vertex, we suspect that the characteristic temperature at which this vertex saturates[4,5] will get larger. This may then remove the problem associated with the U dependence of the Kondo temperature in the Suhl vertex calculations, which Hamann[5] points out goes as

$$T_k \propto e^{-(U/\pi\Delta)^2}$$

instead of the $e^{-U/\pi\Delta}$ expected from the Schrieffer-Wolff transformation.[17]

If this speculation is indeed correct, a finite-width parquet calculation would result in transport properties (e.g., the resistivity ρ) and thermodynamic properties (e.g., c_v) with reasonable temperature dependence for local-moment and Kondo-system effects. A problem would still remain with the susceptibility, however. The self-consistent χ should be weaker than that of the Suhl vertex calculations which, as Hamann[5] has shown, has much too small a Curie constant. A proper calculation of χ would be the conserving approximation, which does too good a job of enhancing the susceptibility in the zero-width approximation. However, in the finite-width calculation we would not be seeking a divergence at exactly $T = 0$; we would expect an enhanced, but finite, self-consistent vertex at $T = 0$, and there is room, at least, to get a still

further enhanced, but finite, conserving susceptibility at $T=0$.

Without doing the calculation, all we may do is speculate what the results will be. However, our experience with the zero-width calculation indicates that the computational problem involved is stupendous. Some approximation, such as a Lorentzian shape to the low-frequency modes,[4,5] will be essential before such a calculation can be contemplated.

ACKNOWLEDGMENTS

We would like to thank Professor M. J. Levine, Dr. T. V. Ramakrishnan, and Professor H. Suhl for many helpful conversations during the course of this research.

[1]H. Suhl, Phys. Rev. Letters 19, 442 (1967); 19, 735 (E) (1967).
[2]P. W. Anderson, Phys. Rev. 124, 41 (1961).
[3]P. A. Wolff, Phys. Rev. 124, 1030 (1961).
[4]M. J. Levine and H. Suhl, Phys. Rev. 171, 567 (1968); M. J. Levine, T. V. Ramakrishnan, and R. A. Weiner, Phys. Rev. Letters 20, 1370 (1968).
[5]D. R. Hamann, Phys. Rev. 186, 549 (1969).
[6]We shall use the notation of the Anderson model in this paper; the results obtained are identical with those based on the Wolff model.
[7]M. T. Béal-Monod and D. L. Mills, Phys. Rev. Letters 24, 225 (1970).
[8]A. A. Abrikosov, Physics 2, 5 (1965); B. Roulet, J. Gavoret, and P. Nozières, Phys. Rev. 178, 1072 (1969).
[9]R. A. Weiner, Phys. Rev. Letters 24, 1071 (1970).
[10]G. Baym and L. P. Kadanoff, Phys. Rev. 124, 287 (1961).
[11]The parquet diagrams are only a formal method of generating all diagrams for the vertex function, since the totally irreducible vertex I must still be obtained by a perturbative expansion.
[12]A. A. Abrikosov, L. P. Gor'kov, and I.-E. Dzyaloshinski, in *Methods of Quantum Field Theory in Statistical Physics*, edited by R. Silverman (Prentice-Hall, Englewood Cliffs, N. J., 1963).
[13]The Bethe-Salpeter equation for γ^{ee} does not generate a narrow low-frequency mode.
[14]The solution to the Suhl vertex equation is roughly proportional to $\delta_{\omega,0}$ at high temperatures (see M. J. Levine and H. Suhl, Ref. 4).
[15]This shifts the effective location of the d-state resonance to $\epsilon=0$ (see Ref. 5).
[16]A similar calculation of the susceptibility in a local-moment model has been reported by J. A. Appelbaum and D. R. Penn, Phys. Rev. B 3, 942 (1971).
[17]J. R. Schrieffer and P. A. Wolff, Phys. Rev. 149, 491 (1966).

PHYSICAL REVIEW B VOLUME 4, NUMBER 9 1 NOVEMBER 1971

Renormalization Group and Critical Phenomena. I. Renormalization Group and the Kadanoff Scaling Picture*

Kenneth G. Wilson
Laboratory of Nuclear Studies, Cornell University, Ithaca, New York 14850
(Received 2 June 1971)

The Kadanoff theory of scaling near the critical point for an Ising ferromagnet is cast in differential form. The resulting differential equations are an example of the differential equations of the renormalization group. It is shown that the Widom-Kadanoff scaling laws arise naturally from these differential equations if the coefficients in the equations are analytic at the critical point. A generalization of the Kadanoff scaling picture involving an "irrelevant" variable is considered; in this case the scaling laws result from the renormalization-group equations only if the solution of the equations goes asymptotically to a fixed point.

The problem of critical behavior in ferromagnets (and other systems) has long been a puzzle.[1] Consider the Ising model of a ferromagnet; the partition function is

$$Z(K,h)=\sum_{\{s\}}\exp\left(K\sum_{\vec{n}}\sum_{i}s_{\vec{n}}\,s_{\vec{n}+\vec{i}}+h\sum_{\vec{n}}s_{\vec{n}}\right), \qquad (1)$$

where $K=-J/kT$, J is a coupling constant, $s_{\vec{n}}$ is the spin at lattice site $\vec{n}$, $\sum_i$ is a sum over nearest-neighbor sites, and h is a magnetic field variable. The spin $s_{\vec{n}}$ is restricted to be ± 1; $\sum_{\{s\}}$ means a sum over all possible configurations of the spins. T is the temperature, and k is Boltzmann's constant. The partition function is a sum of exponentials each of which is analytic in K and h. Therefore one would expect the partition function itself to be analytic in K and h. In fact, however, the partition function is singular for $K=k_c$ and $h=0$, where K_c is the critical value of K. To be precise, the singularity occurs only in the infinite-volume limit, in which case one calculates the free-energy density

$$F(K,h)=\lim_{V\to\infty}\frac{1}{V}\ln Z(K,h), \qquad (2)$$